SCA2003-23: ON THE EFFECT OF RESERVOIR CONFINING STRESS ON MERCURY INTRUSION-DERIVED PORE FREQUENCY DISTRIBUTION

P. Mitchell, Integrated Core Consultancy Services
K. Sincock & J. Williams, BP Exploration

This paper was prepared for presentation at the International Symposium of the Society of Core Analysts held in Pau, France, 21-24 September 2003

ABSTRACT

For many years high-pressure mercury intrusion has been used as a valuable contributor to hydrocarbon reservoir appraisal. As a method for generating drainage capillary pressure information it possesses significant advantages over other methods in terms of the speed of data generation in addition to offering saturation prediction at higher drainage pressures than other methods. The main historical drawback of high-pressure mercury intrusion is that it is performed with the sample unstressed and therefore not representative of downhole conditions.

New data generated for the first time under representative confining stress are presented in this paper for a wide range of rock types. In addition, data are presented showing the effect over the whole pore frequency distribution of progressive stress application from nominal confinement through to reservoir-representative stresses and beyond for specific samples. The transformations observed as a function of increasing confining stress are discussed.

In many cases, substantial changes in key aspects of the pore frequency distribution under stressed conditions have been noted. In particular systematic change in threshold pressure, microporosity content and intergranular pore distribution are typically observed. The impact on important reservoir appraisal parameters such as seal capacity, connate water saturation and transitional behaviour caused by these changes is also discussed.

INTRODUCTION

Historically, mercury intrusion has been used to estimate primary drainage characteristics of reservoir rock samples at low intrusion pressures. In recent times, technology has matured to the point where very high intrusion pressures are routinely used, sufficient to enter essentially all of the connected pore space within rock samples and thus characterise the entire pore frequency distribution of the subject test sample. The major unresolved question has remained the absence of representative confining stress during high-pressure mercury intrusion testing. A complication arising in this respect is that the mercury itself imparts a confining stress on the test sample, specifically acting to compress the uninvaded fraction of the pore space.

The options available to the analyst are to confine the sample with (1) fixed stress, which will correctly confine the whole sample initially and that portion of the sample invaded with mercury during the progress of the test, or (2) variable stress, progressively reduced during testing which will correctly confine the uninvaded portion of the porespace. The latter approach will, however, suffer excess intrusion of mercury into the already mercury-saturated part of the porespace due to sample relaxation whereas the former will not. Both will transiently over-confine the uninvaded porespace at elevated injection pressures, as in the unconfined case. The approach favoured by the authors is to pre-stress the whole sample with a fixed lithostatic confining pressure, which ensures that the total intrusion volume of the sample remains representative of downhole conditions throughout testing.

The primary purpose of this paper is to present new data showing the effect of stress on mercury intrusion-derived pore frequency distributions for a plurality of disparate rock types at a suite of pressures designed to encompass both original downhole stresses and much higher stresses which can pertain to various parts of hydrocarbon reservoirs during exploitation.

EXPERIMENTAL PROCEDURES

A total of six samples were selected for study, representing the following range of classical rock types: limestone, siltstone (caprock), chloritic sandstone, tight gas sandstone, poorly consolidated sandstone and chalk. Each sample was divided into six sub-samples to enable characterisation in the unstressed state and at the following confining stresses: 2000, 4000, 6000, 10000 and 16000 psi hydrostatic. Visual inspection was used to ensure compatibility of all of the samples as far as possible to prevent natural heterogeneity confounding the experimental results. The experimental protocols and subsequent data manipulation essentially conform to well-established methods, very similar to those described by Shafer et al [1]. A total of 122 pre-set pressure increments separated by a constant multiplier ranging from 1.5 psia to 60000 psia intrusion pressure were used. This high density of data points provides for high resolution delineation of the pore frequency distribution regardless of where the modal pore size lies in the pressure sequence.

The samples are confined prior to analysis using a novel miniature pre-stressing system made of very low compressibility materials, which maintains a fixed hydrostatic confining stress on the sample during testing. The whole assembly is designed to fit inside the penetrometer in the normal way. The pressure vessel used is a scaled down version of a typical hydrostatic coreholder. After the application of the desired confining stress, the sleeve fluid solidifies and hardens, thereafter maintaining the same strain on the sample as prior to solidification of the sleeve fluid. The rock sample is protected from invasion of the sleeve fluid prior to hardening by a special membrane sleeve. The testing protocol under stressed conditions is otherwise identical to conventional high-pressure mercury intrusion. Specific penetrometer blank corrections are preferred to minimise systematic errors associated with generalised blank corrections. The

mercury is allowed to access the sample through ports in the confining cell all around the sample. This ensures three-dimensional intrusion, as in the unconfined case, thus eliminating spatial anisotropy since our purpose here is to examine solely the effect of stress on the pore frequency distribution.

RESULTS AND DISCUSSION

Analysis of Data

Given a fluid [mercury] of surface tension g and a material containing pores of diameter D, the capillary pressure P_c that is required for the fluid to invade the material is given by:

$$P_c = k_1 \frac{g \cos j}{D} \qquad \text{Equation 1}$$

where j is the contact angle between the fluid and material and k_1 a unit-dependent constant. The logarithmic pore frequency F is defined by:

$$F\left(D_{i+½}\right) = \frac{v_{i+1} - v_i}{\log_{10}\left(D_{i+1}\right) - \log_{10}\left(D_i\right)} \qquad \text{Equation 2}$$

where v is the cumulative intrusion and D is pore diameter.

If the diameter of the pores is plotted on the x-axis using a logarithmic scale and one decade of the axis is taken as unity, then a scaling factor Z for the y-axis can be defined such that one unit of area under the curve $F(D)$ corresponds to one absolute percentage point of porosity (or "porosity unit"). The factor Z is given by:

$$Z = \frac{f r_B}{v_\infty} = \frac{f r_{gg}}{(1+f) v_\infty} \qquad \text{Equation 3}$$

where $v_¥$ is the total volume of mercury injected, f is the sample fractional porosity, r_B the bulk density and r_{gr} the grain density of the sample.

Using Darcy's law, Poiseuille's equation and Archie's law, a theoretical estimate of sample permeability can be made:

$$K_t = k_2 g_{Hg} \cos j \, f^m \sum_{i=0}^{\infty} D_i^{\,2} \Delta s_i \qquad \text{Equation 4}$$

where m is the Archie cementation exponent, s_i is the mercury saturation ($= v_i/v_\infty$) and k_2 a unit-dependent constant. This theoretically derived permeability value conforms closely on an historical basis [2] with measured Klinkenberg [3] permeability values.

Sample Mineralogies

The mineralogical composition of the samples was determined by X-ray diffraction. The results are given in Table 1:

Table 1: Bulk Mineralogy of Samples Studied (by X-ray Diffraction)

Sample	Description	Composition (%)							
		Mica	Clay	Quartz	Microcline	Plagioclase	Calcite	Siderite	Pyrite
1	Limestone	1					98		1
2	Kimmeridge Clay	4	19	62	4	4	3		4
3	Chloritic Sandstone		5	85	2	8			
4	Tight Gas Sand	1	7	87		3		2	
5	Poorly Consol'd Sand			98	2				
6	Chalk	1		1			98		

The limestone and chalk samples are composed essentially of calcite. The Kimmeridge Clay sample is a clay-rich siltstone. Both the chloritic sand and the tight gas sand contain a significant clay fraction, however the former is rich in diagenetic chlorite, the latter has a mixture of authigenic and detrital clays. The poorly consolidated sand is very close to pure quartz.

Sample-Specific Results

A single page has been devoted to the results for each sample comprising a geological description, pore frequency distribution plots and capillary pressure plots, showing changes as a function of the increasing hydrostatic confining stress regime. A summary table is also presented for each sample showing changes of important sample parameters as a function of applied stress. An interpretation of the results is also given sample by sample.

Sample 1 – Limestone (Original Depth – circa 2300 mtvdss)

Description:- Limestone (Peloidal Packstone). Peloidal grains composed of microsparite. Intergranular cements consist of patchy lime mud (<2 microns) and pervasive early phase grain coating calcite spar crystals. Effective porosity is present between the cement-coated grains themselves (intergranular), and within occasional calcite dissolution vugs. The microsparite peloid grains also contain microporosity.

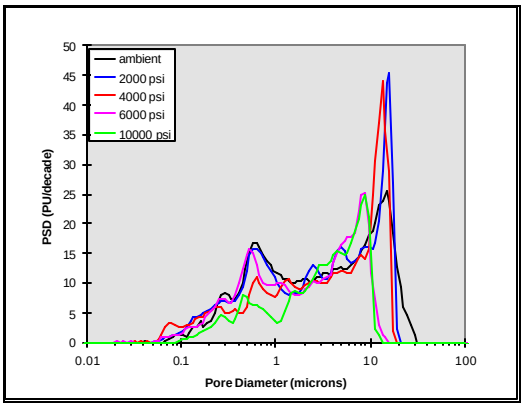

Figure 1 - Pore Size Distribution

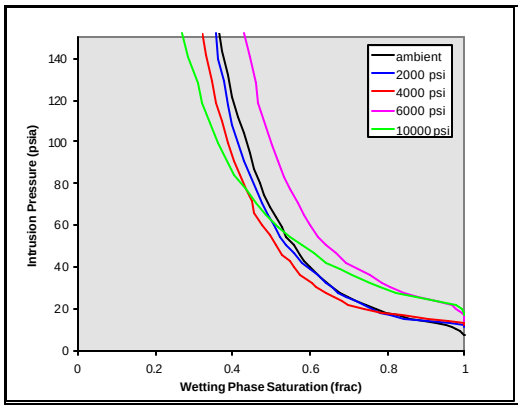

Figure 2 - Capillary Pressure Curves

A general trend of increasing entry pressure is evident with stress together with a reduction in modal pore diameter (Figure 1, Table 2). At high stress, the sample shows signs of collapse, with a large shift in modal pore size and associated loss of permeability. At the final stress a mode of porosity at around 0.5 µm is absent, suggesting destruction of vugs or porous framework grains. The capillary pressure curves at moderate stress cross over the ambient curve as a result of both an increase in entry pressure, coupled with a relative loss of micro-porosity under stressed conditions compared with ambient (Figure 2). This effect is more dramatic at the final stress, where a substantial mode of microporosity no longer exists.

Figure 3 - SEM Micrograph

Table 2 - Sample Properties vs Applied Stress

Applied Stress	Porosity	Theo. Perm.	Modal Pore Diam	Entry Pressure
	frac	mD	µm	psia
Ambient	0.305	211	14.6	1.39
2000	0.313	199	16.0	2.11
4000	0.271	141	13.4	2.32
6000	0.230	37	8.8	2.74
10000	0.169	23	8.8	3.23

Sample 2 – Kimmeridge Clay (Original Depth – circa 2500 mtvdss)

Description:- A clay-rich siltstone with micaceous laminae. Silt grade detrital grains in a clay matrix, the latter comprising 19% of the rock material. Interstitial clays are ductile and will readily deform under confining stress. The silt framework grains are partially silica cemented and will, therefore, afford the rock some mechanical strength at moderate confining stresses.

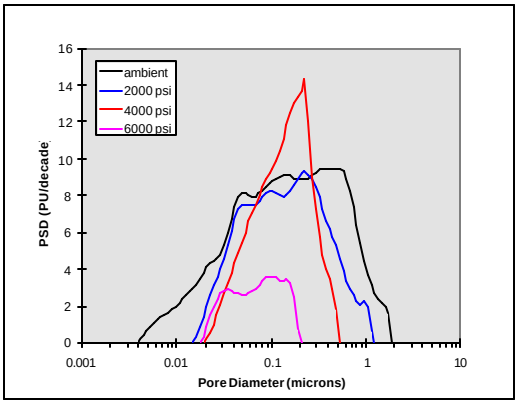

Figure 4 - Pore Size Distribution

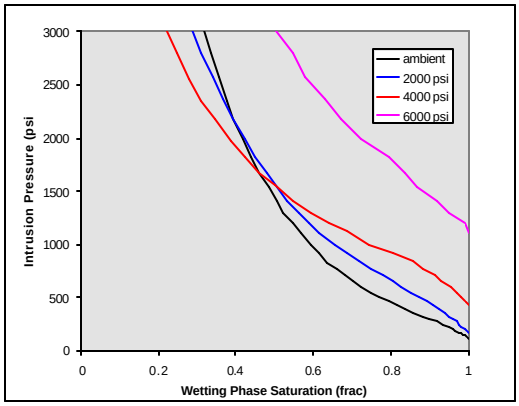

Figure 5 - Capillary Pressure Curves

No testing above 6000 psi took place due to shortage of material. Sample entry pressure increases very significantly at progressive confining stresses (Figure 4, Table 3). A considerable sharpening of the distribution occurs with the application of confining stress, with an increase in entry pressure accompanying loss of microporosity. This consequently results in the 2000 and 4000 psi capillary pressure curves crossing over the ambient curve. The sample collapses at the high final stress, which is evident in the sample summary data in Table 3. Under approximate in-situ stress predicted seal capacity increases by a factor of 3.6 compared with the unstressed determination. This observation is important because the Kimmeridge Clay Formation provides capillary seal for many UK North Sea fields.

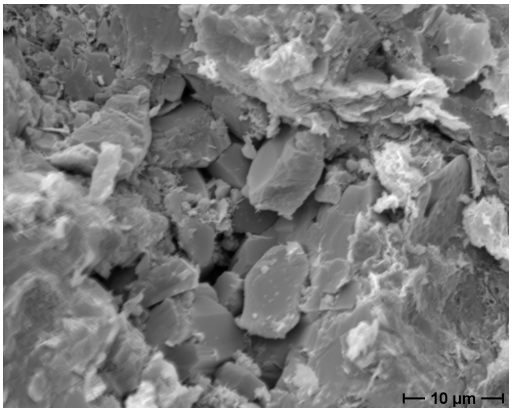

Figure 6 - SEM Micrograph

Table 3 - Sample Properties vs Applied Stress

Applied Stress	Porosity	Theo. Perm.	Modal Pore Diam	Entry Pressure
	frac	mD	µm	psia
Ambient	0.157	0.134	0.53	119
2000	0.106	0.030	0.23	181
4000	0.093	0.0091	0.23	425
6000	0.025	0.0002	0.09	1112

Sample 3 - Chloritic Sandstone (Original Depth – circa 3000 mtvdss)

Description:- Sandstone (Quartz Arenite). Fine grained, moderately to well sorted, well rounded sandstone, with pronounced clay coating (5 microns thickness) of detrital grains. Clay coatings (approximately 5% of rock volume) consist of rosette-habit authigenic chlorite. Porosity consists of microporosity within the clay coats, and intergranular porosity between the clay-coated grains. At stress intergranular porosity will be reduced due to extrusion of clay from contacts between clay-lined grains into pore spaces.

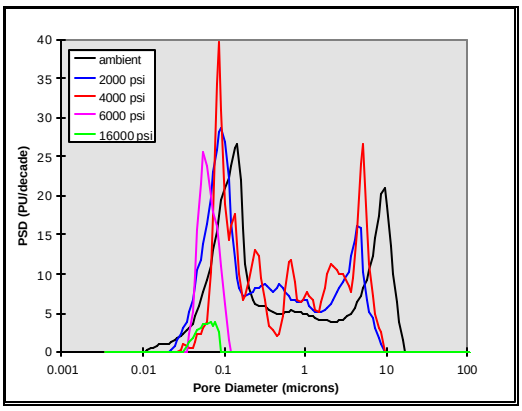

Figure 7 - Pore Size Distribution

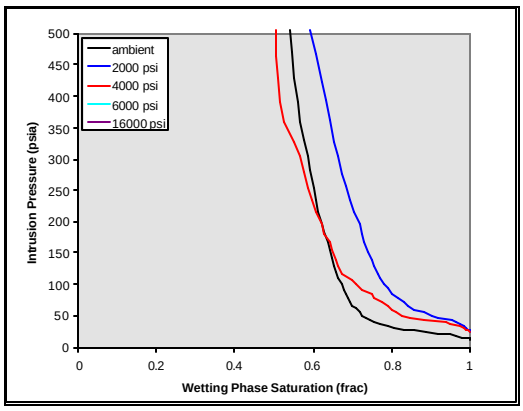

Figure 8 - Capillary Pressure Curves

The sample possesses a strongly bi-modal distribution due to the presence of diagenetic chlorite florets. At moderate stress (4000 psi), there is a sharpening effect on the frequency distribution (Figure 7): an increase in entry pressure and loss of microporosity which increases the contrast or separation between micro and macroporosity. This results in a crossing of the capillary pressure curve at this stress over the ambient curve (Figure 8). At high stress (6000, 16000 psi) complete destruction of intergranular porosity takes place and the intergranular peak disappears. The only remaining porosity is associated with clay rosettes, which is reflected in the enormous increase in entry pressure.

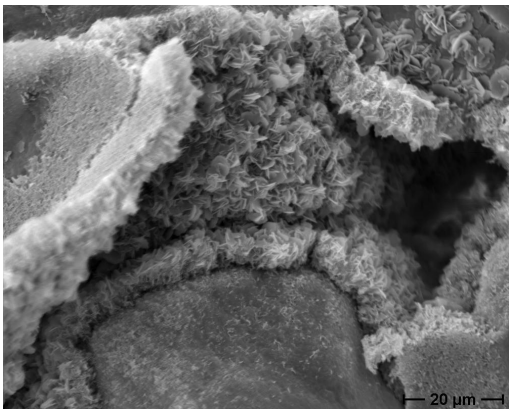

Figure 9 - SEM Micrograph

Table 4 - Sample Properties vs Applied Stress

Applied Stress	Porosity	Theo. Perm.	Modal Pore Diam	Entry Pressure
	frac	mD	µm	psia
Ambient	0.261	48	9.58	12.9
2000	0.258	9	4.41	23.5
4000	0.256	14	5.23	23.5
6000	0.063	0.00055	0.06	1848
16000	0.010	0.00001	0.06	2392

Sample 4 - Tight Gas (Original Depth – circa 2500 mtvdss)

Description:- Sandstone (Quartz Arenite). Very fine grained silty sandstone, grains poorly to moderately sorted, angular to moderately rounded, with moderate clay cement. Intergranular clays (7% of rock volume) are, primarily, illite (mostly platy with occasional fibrous habit) and chlorite (interlocking crystals, frequently exhibiting rosette habit). Porosity consists of significant microporosity within the clay cements and also intergranular porosity between the clay cemented detrital grains.

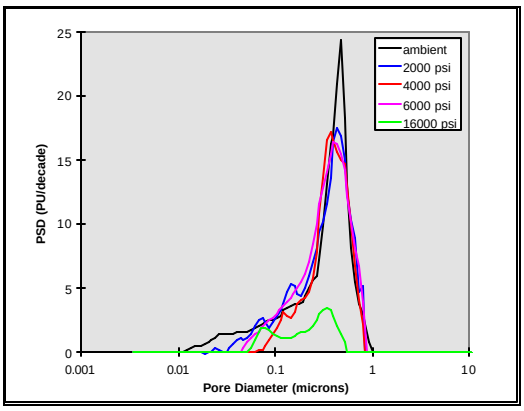

Figure 10 - Pore Size Distribution

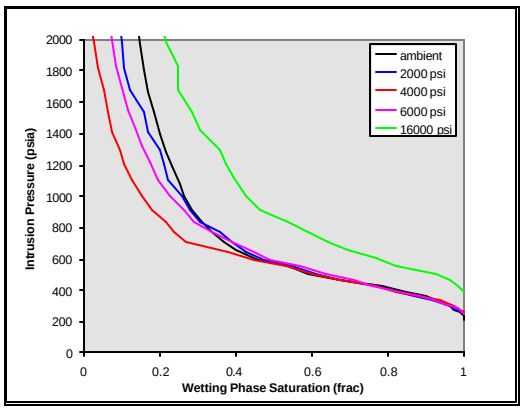

Figure 11 - Capillary Pressure Curves

The mechanical hardness of the sample is reflected in the near-impervious nature of both modal pore size and entry pressure to the application of progressive confining stress (Figure 10, Table 5). Microporosity is significantly affected, however, and the loss of microporosity at moderate stresses is manifested in the separation of the capillary pressure curves at low wetting phase saturations (Figure 11). At the very high final stress of 16000 psi, the sample finally collapses, causing a large increase in entry pressure to mercury and the near-annihilation of permeability and porosity.

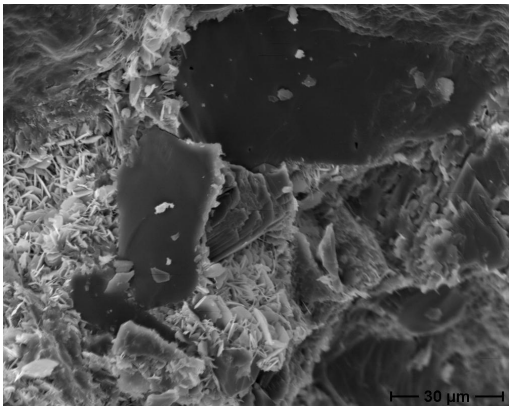

Figure 12 - SEM Micrograph

Table 5 - Sample Properties vs Applied Stress

Applied Stress	Porosity	Theo. Perm	Modal Pore Diam	Entry Pressure
	frac	mD	µm	psia
Ambient	0.083	0.035	0.48	215
2000	0.079	0.032	0.45	256
4000	0.070	0.026	0.38	256
6000	0.080	0.033	0.41	255
16000	0.015	0.001	0.32	391

Sample 5 - Poorly Cemented Sandstone (Original Depth – circa 2600 mtvdss)

Description:- Sandstone (Extremely Weakly Cemented Quartz Arenite). Generally fine to medium grained, poorly to moderately sorted, moderately to well rounded (occasional subangular grains). Grains composed almost entirely of quartz, with only a very few grains exhibiting any form of cementation at point contacts (rare, weak silica cementation).

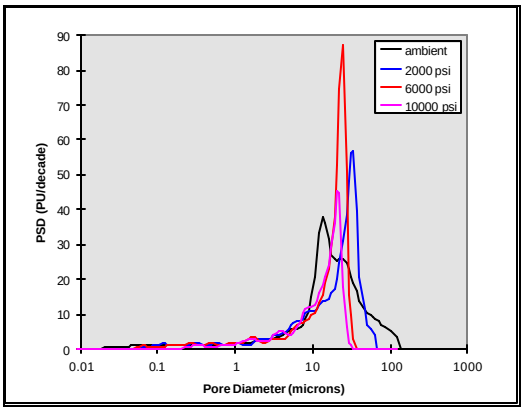

Figure 13 - Pore Size Distribution

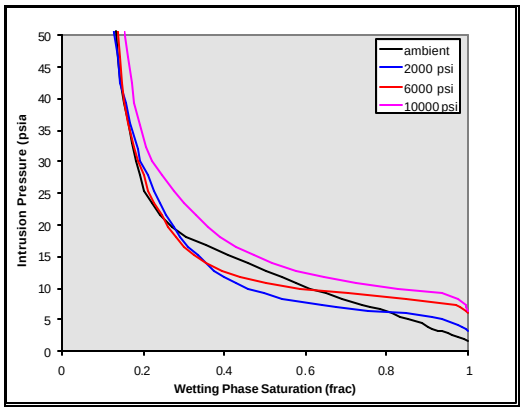

Figure 14 - Capillary Pressure Curves

Two tests failed and could not be repeated due to shortage of material. The ambient frequency distribution curve reflects the poorly consolidated nature of the sample, with compaction of the sample by mercury in the early stages of the test manifesting itself as false intrusion (Figure 13). The test at 2000 psi correctly illustrates the unimodal nature of the pore system under representative confinement. At progressively higher stress, the distribution continues to sharpen prior to blunting at the top stress due to the sample yielding mechanically. The false intrusion in the ambient experiment translates to a large artefact in the transitional properties of the sample as shown in Figure 14. The capillary pressure curves at moderate stress cross over the ambient curve in the mid-range prior to converging at higher intrusion pressures. This reflects the absence of microporosity.

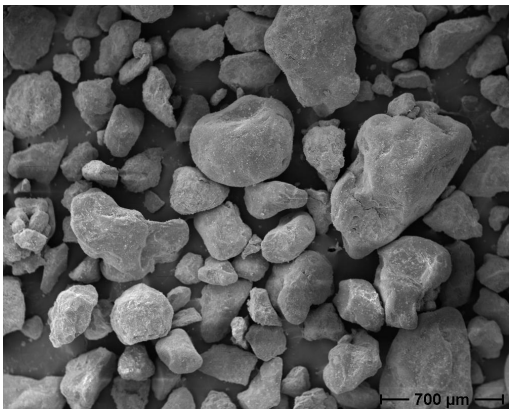

Figure 15 - SEM Micrograph

Table 6 - Sample Properties vs Applied Stress

Applied Stress	Porosity	Theo' Perm	Modal Pore Diam	Entry Pressure
	frac	mD	µm	psia
Ambient	0.285	2743	13.4	1.6
2000	0.263	1443	34.1	3.4
6000	0.244	674	24.4	6.1
10000	0.158	187	20.7	6.6

Sample 6 – Chalk (Original Depth – circa 2800 mtvdss)

Description:- Chalk (Micritic Wackestone). Chalk is weakly cemented, and composed of both whole and fragmented coccoliths (whole specimens 5-7 microns diameter) and rare planktonic foraminiferans (50 microns test diameter) in a finely crystalline calcite spar (1-2 microns) matrix. Effective porosity is dominantly within the micropores of the microcrystalline calcite spar matrix. Intra-skeletal pores are rarely connected.

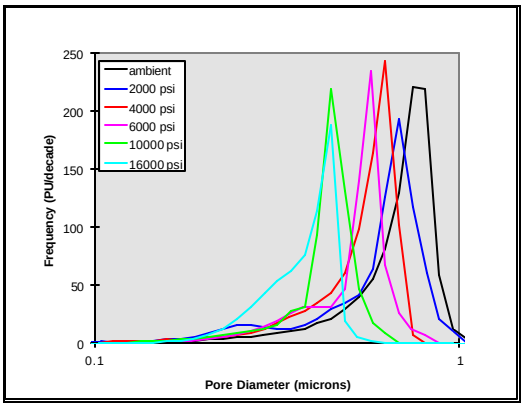

Figure 16 - Pore Size Distribution

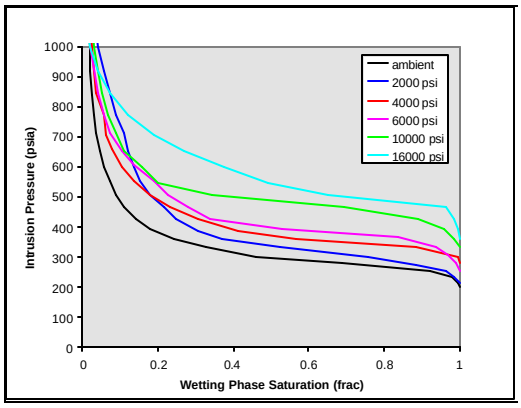

Figure 17 - Capillary Pressure Curves

This sample exhibits the sharply unimodal pore frequency distribution often associated with chalks (Figure 16). The behaviour of the sample at progressive stress is highly systematic, with near-linear change in modal pore size and entry pressure (Table 7). The consistency in the morphology of the frequency distributions is repeated in the capillary pressure curves (Figure 17), which essentially shift upwards monotonically as a function of confining stress. The sample shows no sign of sudden or even incipient failure at high stress, and is the only sample tested which falls into this category. This behaviour could be explained by the rather open cage-like structure of the rock, which is able to deform readily in response to applied stress.

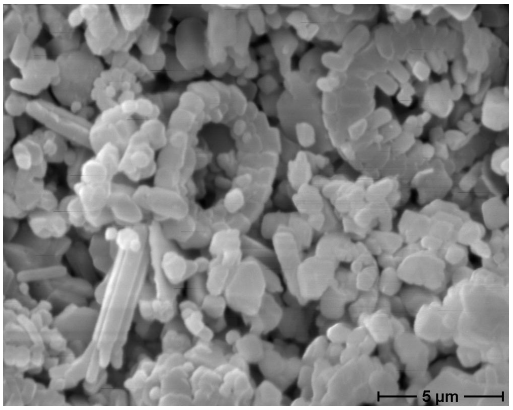

Figure 18 - SEM Micrograph

Table 7 - Sample Properties vs Applied Stress

Applied Stress	Porosity	Theo' Perm	Modal Pore Diam	Entry Pressure
	frac	mD	µm	psia
Ambient	0.428	2.73	0.742	197
2000	0.369	1.61	0.682	215
4000	0.381	1.36	0.626	279
6000	0.285	0.67	0.570	257
10000	0.260	0.40	0.445	330
16000	0.253	0.29	0.443	360

Sample 7 – Synthetic Sample

A synthetic sample chosen for its very high homogeneity was selected for study to demonstrate accuracy and reproducibility of mercury intrusion under confining stress. The sample was known to be mechanically hard with very low compressibility as determined by helium expansion at ambient and under hydrostatic confinement.

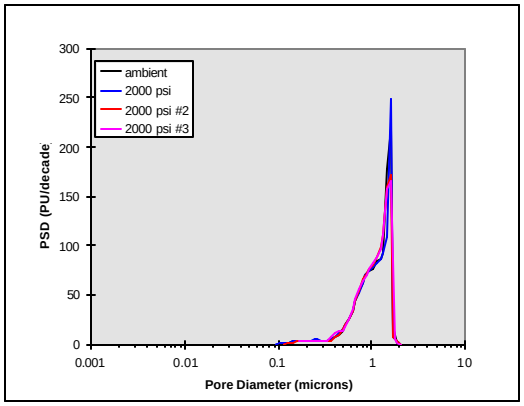

Figure 19 - Pore Size Distribution (2000 psi)

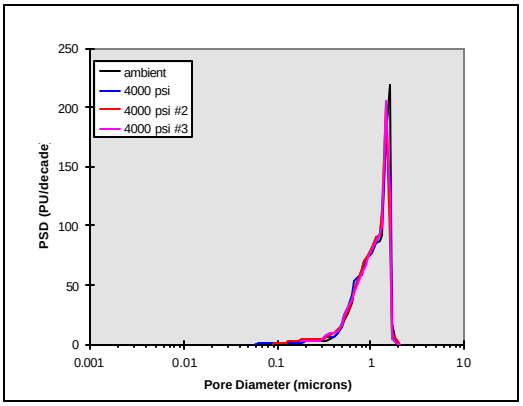

Figure 20 – Pore Size Distribution (4000 psi)

Table 8 - Sample Properties vs Applied Stress

Applied Stress	Porosity	Helium Porosity	Theo. Perm.	Modal Pore Diam	Entry Pressure
	frac	frac	mD	µm	psia
Ambient	0.462	0.460	9.15	1.58	110
2000	0.451	0.458	8.71	1.60	109
2000 #2	0.454	-	8.65	1.60	109
2000 #3	0.459	-	8.64	1.60	109
4000	0.454	0.457	8.36	1.47	109
4000 #2	0.451	-	7.91	1.47	110
4000 #3	0.449	-	8.14	1.47	110

Comparison of the frequency distribution measured unconfined is made with those repeatedly determined (after sub-sampling) at 2000 and 4000 psi in Figures 19 and 20 respectively. There is minimal change in the frequency distribution at either confining stress – all functions essentially overplot the ambient curve. Summary data are given in Table 8. The uncertainty under given conditions in total intrusion volume appears to be in the region of 1% (relative) which is much lower than the changes with stress typically observed in the reservoir rock samples. The non-monotonic behaviour occasionally seen in the other samples studied also exceeds this in magnitude, which is suggestive of heterogeneity as the cause. The slightly greater change in porosity with stress determined by mercury compared with helium could hint at reduced accessibility of microporosity to mercury under stressed conditions. This phenomenon may

account for some of the microporosity loss observed by mercury at stress for the reservoir rock samples.

CONCLUSIONS

The database of mercury intrusion data accrued to date and presented in this paper supports the following inferences:

1. Sample entry pressure increases monotonically as a function of confining stress. This means that traditional mercury intrusion methods will underestimate the seal capacity of caprock samples.

2. Mercury intrusion data for poorly consolidated materials are artefacted by compaction of the sample at low intrusion pressures. Confinement of the sample at reservoir-representative stress overcomes this problem.

3. Relatively higher loss of microporosity compared to macroporosity is a frequent observation under representative stressed conditions. This will result in prediction of lower wetting phase saturations in hydrocarbon zones compared to unstressed mercury intrusion measurements.

ACKNOWLEDGEMENTS

The authors wish to acknowledge BP for granting permission to publish the data contained in this paper. We would like to thank Dr Bruce Sellwood of the University of Reading who performed the petrographic analyses, and the valuable mathematical and other input from Mr. Martin Vlietstra during the preparation of the manuscript is also acknowledged.

REFERENCES

[1] Shafer, J., and Neasham, J.: "Mercury Porosimetry Protocol for Rapid Determination of Petrophysical and Reservoir Quality Properties", *International Symposium of the Society of Core Analysts*, (2000) SCA 2021.

[2] Purcell, W. R.: "Capillary Pressures – Their Measurement Using Mercury and the Calculation of Permeability Therefrom", *Trans. AIME*, (1949).

[3] Klinkenberg, L.J.: "The Permeability of Porous Media to Liquids and Gases", *API Drilling and Production Practices*, (1941) **200**.